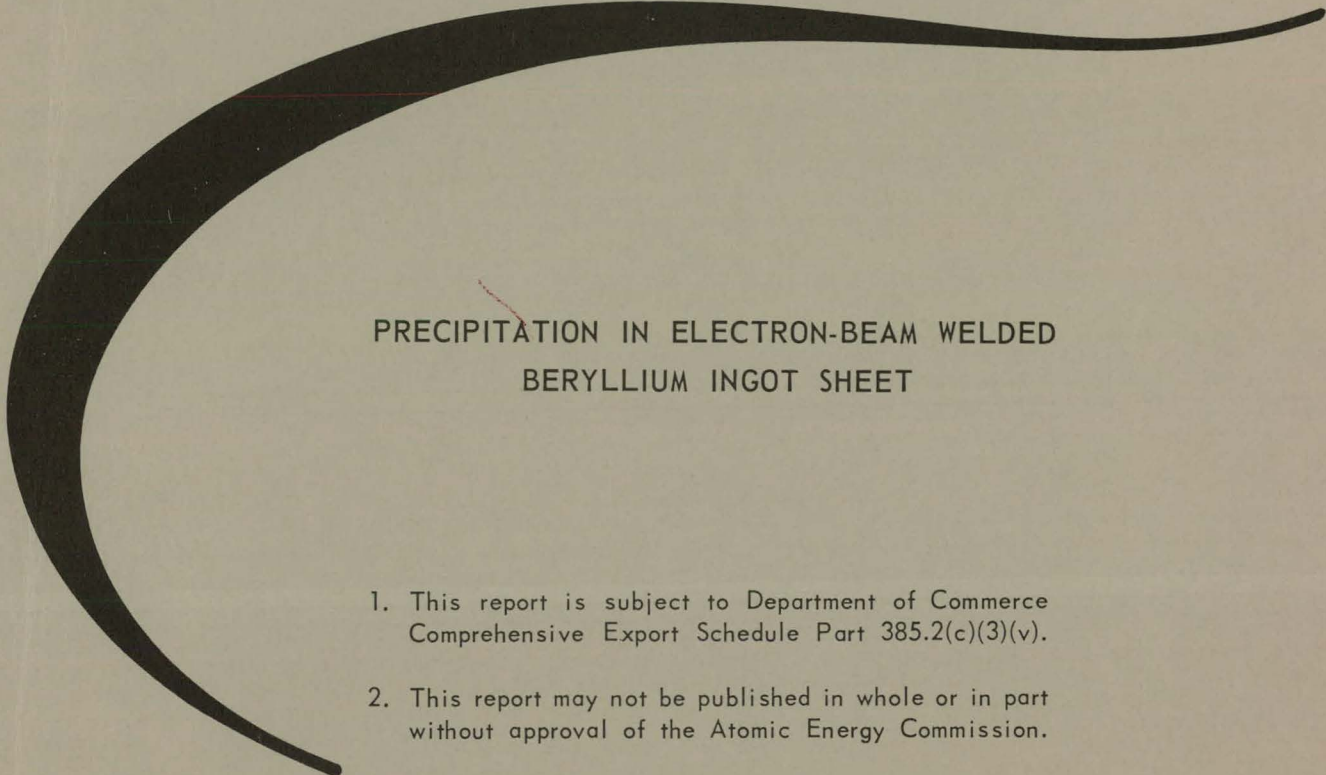


227  
10/24/68  
RFP-1112

*fly*

492

MASTER



PRECIPITATION IN ELECTRON-BEAM WELDED  
BERYLLIUM INGOT SHEET

1. This report is subject to Department of Commerce Comprehensive Export Schedule Part 385.2(c)(3)(v).
2. This report may not be published in whole or in part without approval of the Atomic Energy Commission.



THE DOW CHEMICAL COMPANY  
ROCKY FLATS DIVISION  
P. O. BOX 888  
GOLDEN, COLORADO 80401  
U. S. ATOMIC ENERGY COMMISSION  
CONTRACT AT(29-1)-1106

~~DISTRIBUTION OF THIS DOCUMENT IS UNLIMITED~~

~~DISTRIBUTION OF THIS DOCUMENT IS LIMITED  
Subject to Export Control Domestic  
Distribution Only, Minus Sales Outlets~~



## DISCLAIMER

**This report was prepared as an account of work sponsored by an agency of the United States Government. Neither the United States Government nor any agency Thereof, nor any of their employees, makes any warranty, express or implied, or assumes any legal liability or responsibility for the accuracy, completeness, or usefulness of any information, apparatus, product, or process disclosed, or represents that its use would not infringe privately owned rights. Reference herein to any specific commercial product, process, or service by trade name, trademark, manufacturer, or otherwise does not necessarily constitute or imply its endorsement, recommendation, or favoring by the United States Government or any agency thereof. The views and opinions of authors expressed herein do not necessarily state or reflect those of the United States Government or any agency thereof.**

## **DISCLAIMER**

**Portions of this document may be illegible in electronic image products. Images are produced from the best available original document.**

## LEGAL NOTICE

This report was prepared as an account of Government sponsored work. Neither the United States, nor the Commission, nor any person acting on behalf of the Commission:

A. Makes any warranty or representation, expressed or implied, with respect to the accuracy, completeness, or usefulness of the information contained in this report, or that the use of any information, apparatus, method, or process disclosed in this report may not infringe privately owned rights; or

B. Assumes any liabilities with respect to the use of, or for damages resulting from the use of any information, apparatus, method, or process disclosed in this report.

As used in the above, "person acting on behalf of the Commission" includes any employee or contractor of the Commission, or employee of such contractor, to the extent that such employee or contractor of the Commission, or employee of such contractor prepares, disseminates, or provides access to, any information pursuant to his employment or contract with the Commission, or his employment with such contractor.

September 18, 1968

RFP-1112  
UC-25 METALS, CERAMICS,  
AND MATERIALS  
TID-4500

PRECIPITATION IN ELECTRON-BEAM WELDED  
BERYLLIUM INGOT SHEET

*Frederick J. Fraikor*

*Grant K. Hicken*

*Virgil K. Grotzky*

**LEGAL NOTICE**

This report was prepared as an account of Government sponsored work. Neither the United States, nor the Commission, nor any person acting on behalf of the Commission:

A. Makes any warranty or representation, expressed or implied, with respect to the accuracy, completeness, or usefulness of the information contained in this report, or that the use of any information, apparatus, method, or process disclosed in this report may not infringe privately owned rights; or

B. Assumes any liabilities with respect to the use of, or for damages resulting from the use of any information, apparatus, method, or process disclosed in this report.

As used in the above, "person acting on behalf of the Commission" includes any employee or contractor of the Commission, or employee of such contractor, to the extent that such employee or contractor of the Commission, or employee of such contractor prepares, disseminates, or provides access to, any information pursuant to his employment or contract with the Commission, or his employment with such contractor.

THE DOW CHEMICAL COMPANY  
ROCKY FLATS DIVISION  
P. O. BOX 888  
GOLDEN, COLORADO 80401  
U. S. ATOMIC ENERGY COMMISSION  
CONTRACT AT(29-1)-1106

~~DISTRIBUTION OF THIS DOCUMENT IS UNLIMITED~~

~~DISTRIBUTION OF THIS DOCUMENT IS LIMITED~~  
~~Subject to Export Control Domestic~~  
~~Distribution Only, Minus Sales Outlets~~



**CONTENTS**

Abstract.....	1
Introduction.....	1
Experimental Procedure .....	2
Results and Discussion .....	3
Unaffected Zone .....	4
Partly Recrystallized Zone.....	5
Recrystallized Zone.....	6
Fusion Zone .....	9
Conclusions .....	14
References .....	15

### ACKNOWLEDGMENTS

The authors express appreciation and thanks to W. Booco, H. E. Reed, and D. H. Riefenberg for their valuable assistance.



## PRECIPITATION IN ELECTRON-BEAM WELDED BERYLLIUM INGOT SHEET

*Frederick J. Fraikor, Grant K. Hicken, and Virgil K. Grotzky*

**Abstract.** An investigation was conducted to observe the types, morphology, and behavior of impurity precipitates in beryllium ingot sheet which had been welded by an electron-beam technique. Optical and electron metallography revealed a clear structural transition between the various weld zones. Transmission electron microscopy of the unaffected zone showed dislocation subboundaries 1 to 10 microns in diameter with  $\text{AlFeBe}_4$  precipitates both in the matrix and subboundaries. In areas where the localized weld heating produced temperatures in excess of 900 °C followed by moderate cooling, aluminum-rich grain boundary precipitates were found. Electron-microprobe scanning of weld cracks revealed that these aluminum-rich precipitates introduce hot-short liquid areas which, combined with thermal stresses, produce intergranular cracks.

Transmission photomicrographs further showed that the solidification bands consisted of rows of both irregular shaped  $\text{AlFeBe}_4$  precipitates and platelets of  $\text{FeBe}_{11}$  interconnected by dislocation subboundaries. It is postulated that these solidification bands are produced by solidification fluctuations with resultant microsegregation of iron and aluminum.

### INTRODUCTION

Considerable attention has been focused recently on the joining of beryllium, since this material has found increasing applications, particularly in aerospace and nuclear fields. A review of the techniques, problems, and successes associated with the joining of beryllium can be found in recent reports and articles such as those by Hicken (1) and Hauser (2,3).<sup>1</sup>

Hauser and coworkers (2), for example, have demonstrated the role of varying beryllium-oxide content on the formation of sound electron-beam welds. They found that reducing the beryllium oxide in the starting material consistently reduced the amount

of undercutting, porosity, and surface roughness of the welds. Furthermore, in a similar investigation Hauser and Monroe (3) found indications of extensive precipitation in some of the weld areas and felt that intergranular cracking could be related to grain-boundary precipitation. However, they were unable to make any positive identification of the precipitates or their exact relation to the microstructure.

At the same time, other studies (4 through 11) have demonstrated the role of various impurities, particularly iron and aluminum in precipitation reactions in beryllium. The predominant precipitates in the microstructure of commercial purity beryllium are of the ternary type,  $\text{AlMBe}_4$ , and the binary type,  $\text{MBe}_{11}$ . The  $M$  in the formula is one of the transition elements: iron (Fe), chromium (Cr), nickel (Ni), or manganese (Mn). The precipitation characteristics are dependent on the impurity content and the heat treatment history of each particular beryllium lot. In the case of beryllium ingot sheet currently produced at Rocky Flats, the predominant metallic impurity element is Fe so that  $\text{AlFeBe}_4$  and  $\text{FeBe}_{11}$  are the resultant types of precipitates generally observed in the microstructure. Hence, it appeared feasible to make a comparison of the precipitation characteristics of Rocky Flats beryllium ingot sheet after various heat treatments (10,11,12) with those observed in the various zones of an electron-beam welded sample of the same origin. Furthermore, the oxide content of this ingot sheet is extremely low (0.055 weight percent by neutron-activation analysis). Thus, the problems associated with beryllium oxide in the weld metal as noted by Hauser would be minimized.

The objective of the current investigation was, therefore, to observe the types, morphology, and behavior of impurity precipitates in the microstructure of electron-beam welded beryllium specimens. It should be emphasized that no attempt was made to optimize the welding parameters and the resultant welds. Instead, a variety of welds were produced including samples with wide fusion and heat-affected zones similar to those produced in gas-tungsten-arc welds.

<sup>1</sup> See references at end of text.

## EXPERIMENTAL PROCEDURE

The material utilized in this investigation was 0.225-inch thick Be ingot sheet, rolled from vacuum-cast ingots at the Rocky Flats Division of The Dow Chemical Company. The chemical analysis of the Be sheet is shown in Table I. The sheet was in the as-rolled condition with no post-rolling heat treatments. However, the surface had been chemically etched to remove surface oxides and rolling lubricants.

A high voltage, 6-kilowatt (kw), electron-beam welder was used to make bead on plate welds on the Be sheet. Although a variety of weld sizes was produced, the specimens with exaggerated weld zones were particularly useful for subsequent examination by transmission electron microscopy. The welding parameters used in this instance were an accelerating voltage of 130 kilovolts (kv) with a beam current of 40 milliamperes (ma) and a part velocity of 20 inches per minute (ipm) in a vacuum of  $5 \times 10^{-5}$  torr. The beam-spot size was 0.220 inches in diameter and was focused at approximately  $\frac{1}{8}$  inch below surface. These welding conditions produced intense heating over a wide area with such shallow penetration that the depth-to-width ratio was only 1:1. A cross section of a weld with exaggerated weld zones and cracks is shown in the optical photomicrograph of Figure 1. Other welds

with depth-to-width ratios greater than 3:1 apparently produced crack free welds but the heat-affected zone was too narrow for effective metallographic examination. Little porosity was noted in any of the specimens.

FIGURE 1. Cross Section of Electron-Beam Weld on 0.225-Inch Beryllium Ingot Sheet. Note the Centerline Crack (arrow). (Polarized Light.)

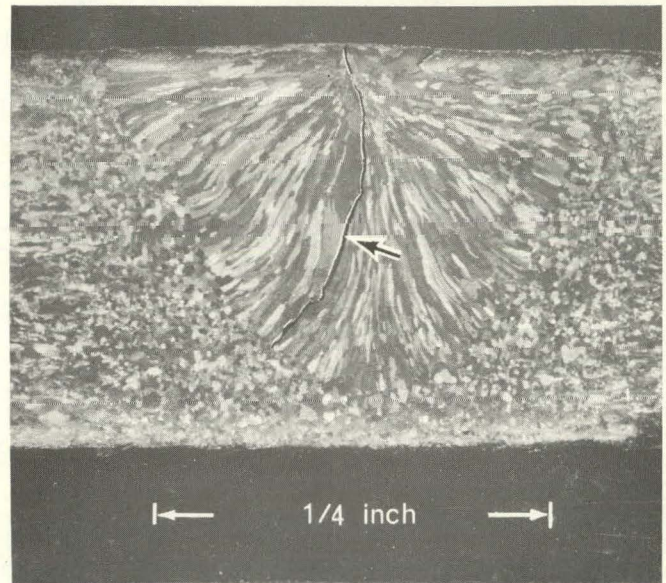


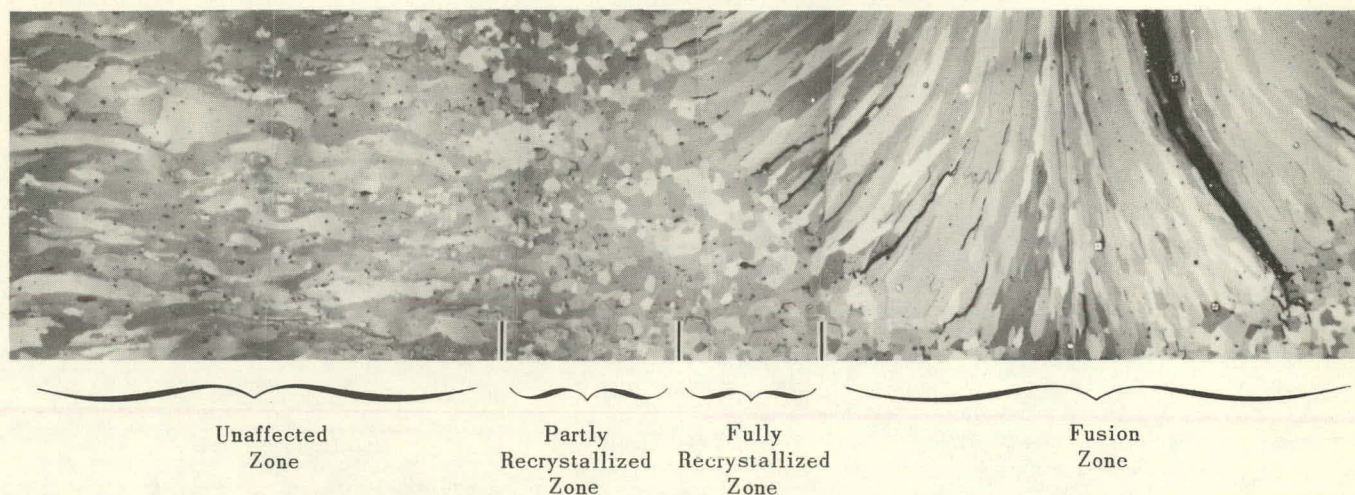
TABLE I. Analysis of 0.225-Inch Thick Beryllium Ingot Sheet.

Impurity	Original Analysis Lot No. 176 CN (weight percent)	Second Analysis Lot No. 176 CN (weight percent)	Third Analysis Lot No. 176 CN (weight percent)
Aluminum (Al)	0.050	0.080	0.060
Beryllium Oxide (BeO)	* 0.26	** 0.055	
Carbon (C)	* 0.065		
Calcium (Ca)	<0.001	0.008	0.003
Cadmium (Cd)	<0.001	0.008	<0.001
Cobalt (Co)	<0.001	0.001	<0.001
Chromium (Cr)	0.015	0.020	0.015
Copper (Cu)	0.020	0.050	0.008
Iron (Fe)	* 0.185	0.250	0.150
Magnesium (Mg)	0.004	0.007	0.002
Manganese (Mn)	0.018	0.013	0.025
Molybdenum (Mo)	<0.001	<0.001	<0.001
Nitrogen (N)	* 0.006		
Nickel (Ni)	0.025	0.013	0.025
Lead (Pb)	0.001	0.002	<0.001
Silicon (Si)	0.060	0.070	0.050
Titanium (Ti)	0.020	0.039	0.010
Tungsten (W)	<0.010	<0.010	<0.010
Zinc (Zn)	<0.010	<0.010	<0.010

\* Chemical analysis; all others by spectroscopic analysis.

\*\* Neutron activation analysis.

FIGURE 2. Optical Photomicrograph Showing Various Weld Zones across Transverse Cross Section of an Electron-Beam Welded Beryllium Sheet Specimen. (Polarized Light.)



The metallographic techniques employed for optical examination of the weld microstructures included illumination by both bright-field and polarized light. Specimens to be examined by polarized light were sectioned by a diamond saw or chemical saw, mounted and rough-ground through 600-grit silicon carbide paper using water as a lubricant. Polishing was continued down through 1-micron diamond paste on a Nylon cloth with deodorized kerosene lubricant and subsequently placed on a Syntron<sup>2</sup> for final polishing overnight with 0.03-micron alumina on a Gamel<sup>3</sup> cloth. The lubricant for final polishing was a slurry of 10 milliliters (ml) of chromic acid in 600 ml of water. The final step was not used for specimens which were to be subjected to electron-microprobe analysis because of the possibility of alumina contamination in voids, cracks, etc.

Although polarized-light illumination successfully revealed the transition between the various weld zones (Figure 2), bright-field illumination of electrolytically polished and etched specimens was necessary to clearly resolve the substructure in some portions of the weld. Details of the technique can be found in Reference 13, Grotzky and Fraikor.

The most difficult portion of the metallographic techniques was the preparation of thin films from

the weld for transmission electron microscopy, particularly since various zones of the weld tend to thin electrolytically at varying rates. To some extent, the problem was solved by masking selected areas on the face of the specimen with lacquer, thus thinning only the desired portion of the weld sample. The electrolytic thinning was accomplished in a Glenn Dual Jet<sup>4</sup> thinning unit using an electrolyte of 400-ml ethylene glycol, 40 ml of nitric acid ( $\text{HNO}_3$ ), 8 ml of sulfuric acid ( $\text{H}_2\text{SO}_4$ ), and 8 ml of hydrochloric acid ( $\text{HCl}$ ), with a current of approximately 900 ma at 36 volts. The electrolyte was kept at a temperature of 10 to 15 °C by a surrounding ice-water bath.

The thin foils were then immersed in hot distilled water, rinsed in methyl alcohol, and then mounted between 75-mesh copper grids and examined at 100 kv in a Phillips<sup>5</sup> EM-200 electron microscope.

## RESULTS AND DISCUSSION

Optical and electron metallography revealed a clear structural transition in some specimens between the various weld zones as illustrated in the low magnification photograph of Figure 2. Beginning with the unaffected zone at the edge of the Be sheet, the specimen exhibited the expected correlation between the temperature gradient and the microstructure.

<sup>2</sup> Syntron Company, Homer City, Pennsylvania.

<sup>3</sup> Fisher Scientific Company, St. Louis, Missouri.

<sup>4</sup> Commercially available from Glenn Electronics and Mechanical Specialties, Inc., Jeannette, Pennsylvania.

<sup>5</sup> North American Phillips Company, Mt. Vernon, New York.

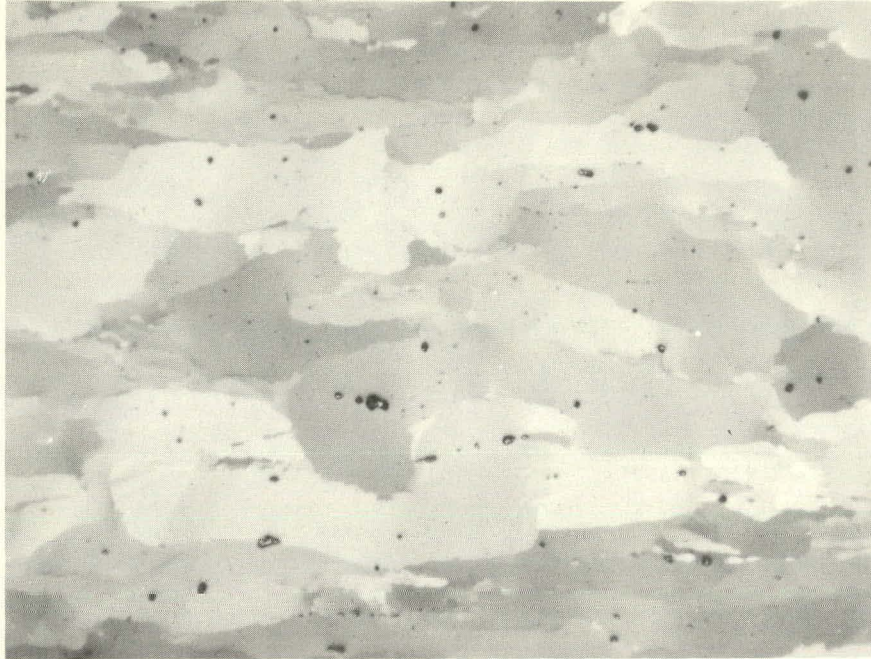


FIGURE 3. Optical Photomicrograph of the Unaffected Zone. Note the Elongated Microstructure of the As-Rolled Beryllium Ingot Sheet. (Polarized Light, Magnification 100X.)

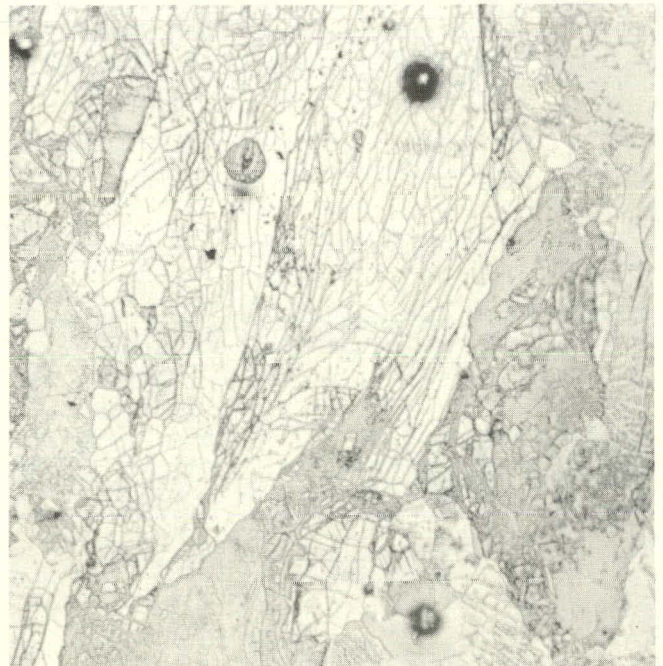
#### Unaffected Zone:

The as-rolled condition of the unaffected portions of the weld samples consisted of a *warm-worked* substructure of dislocation cell walls and subboundaries (Figures 3, 4, and 5). Such a microstructure is the result of rolling the beryllium sheet slightly below the recrystallization temperature so that little or no recrystallization occurs during and after the final rolling pass. The subgrains are 1 to 10 microns in diameter, although the size varies depending on the thermal and rolling history of each particular billet.

In addition to the cellular structure, globular-shaped precipitates 500 to 5000 angstroms ( $\text{\AA}$ ) in diameter are found scattered intermittently throughout the microstructure of the unaffected zone (Figure 5). These particles were identified by electron-diffraction techniques (11) as mainly of the ternary type termed  $\text{AlFeBe}_4$  by Carrabine (8) or  $\text{Be}_5$  ( $\text{Fe, Al}$ ) by Rooksby (7) with a face-centered cubic lattice parameter of approximately  $6.05 \text{ \AA}$ .

The microstructure of the unaffected zone of the beryllium ingot sheet then, can be characterized

FIGURE 4. Optical Photomicrograph of the Unaffected Zone Showing the Subboundaries of the As-Rolled Microstructure. (Bright Field, Magnification 300X.)



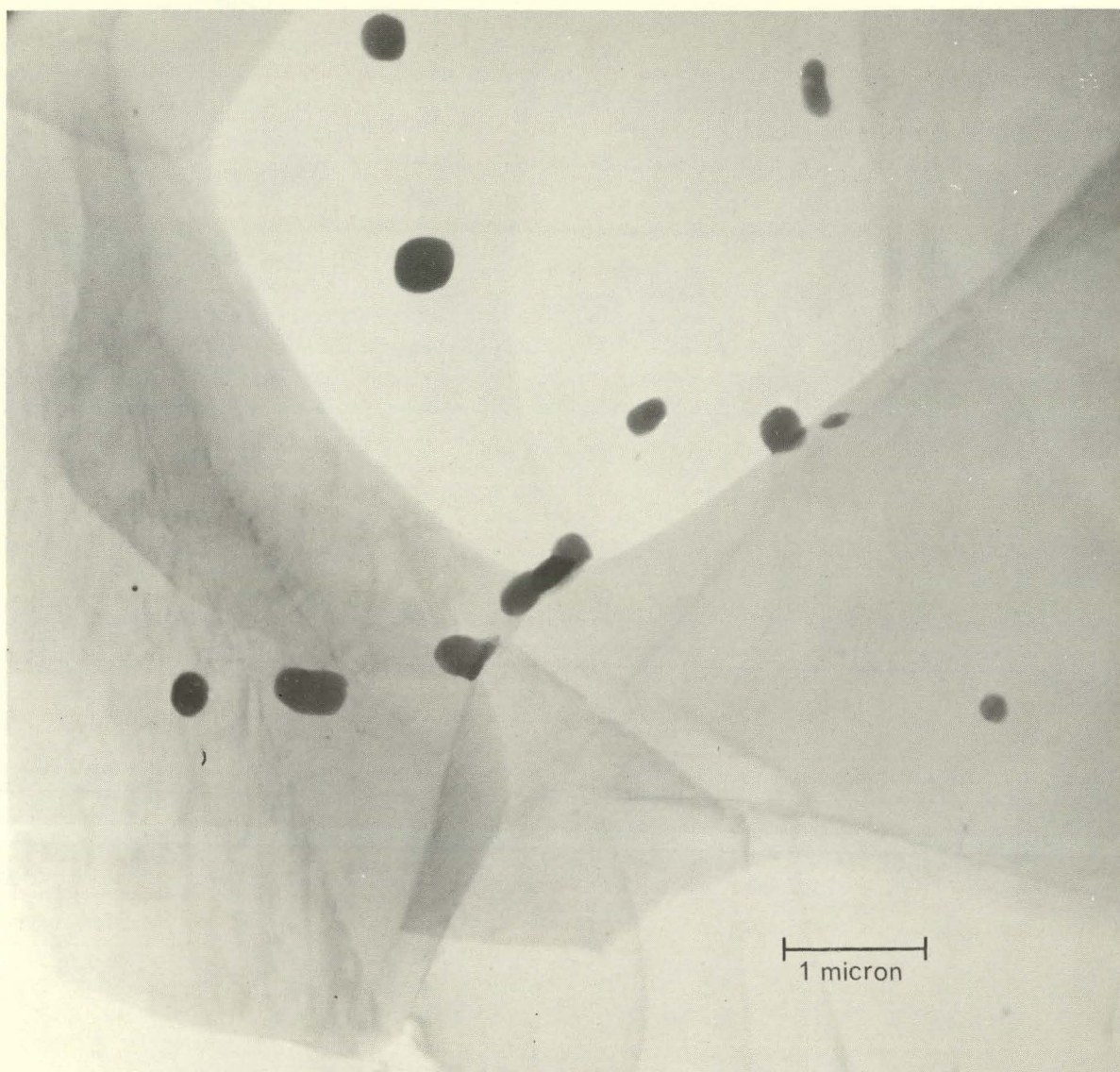


FIGURE 5. Transmission Electron Photomicrograph of the Unaffected Zone of the Beryllium Ingot Sheet. Note the Dislocation Subboundaries and the Globular-Shaped  $\text{AlFeBe}_4$  Precipitates.

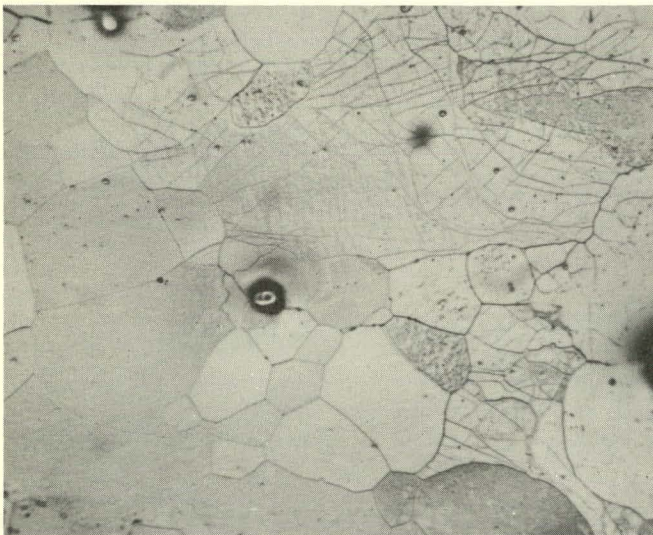
as consisting of dislocation subboundaries with incoherent, globular  $\text{AlFeBe}_4$  precipitates scattered throughout this warm-worked structure. It should be pointed out that Rocky Flats beryllium ingot sheet is generally supplied in the annealed condition; that is, the sheet has undergone a 15 to 20 hour anneal at around  $780^\circ\text{C}$ . In this case, complete recrystallization occurs to a grain size of 40 to 60 microns and some precipitates coalesce to larger sizes (11). Lesser annealing times or lower temperatures produce recovered and partly recrystallized microstructures. Such heat treatment approximately corresponds to the first heat-affected zone of the electron-beam weld.

#### Partly Recrystallized Zone:

Figures 6 and 7 show the microstructure of the partly recrystallized area of the weld specimen. Figure 6 is an optical photomicrograph taken under bright-field illumination and the etch clearly shows some new equiaxed grains among the as-rolled substructure. The transmission electron photomicrograph in Figure 7 further reveals that recovery by the process polygonization has taken place in the remaining as-rolled substructure. That is, sufficient thermal energy was provided at this weld perimeter to allow the dislocations to migrate into narrower cell walls and to assume

more metastable equilibrium configurations in the form of regular arrays. Precipitation in this area was not greatly affected by the electron-beam heating, although the existing precipitates do tend to inhibit boundary migration in some instances. However, closer to the weld where temperatures in excess of 900 °C were achieved, complete recrystallization and grain growth were accompanied by significant changes in the precipitates.

FIGURE 6. Partly Recrystallized Zone. Note the Equiaxed Recrystallized Grains among the Substructure of the As-Rolled Beryllium Ingot Sheet. (Bright Field, Magnification 300X.)



← Toward Fusion Zone      Partly Recrystallized Zone      → Toward Unaffected Zone

#### Recrystallized Zone:

Complete recrystallization in the heat-affected zone resulted in a grain size of approximately 40 to 75 microns in size (Figure 8, Optical Photomicrograph). More significant was the appearance of aluminum-rich precipitates, particularly in the grain boundaries as shown in the transmission electron photomicrograph in Figure 9. In most instances these precipitates are much too small (less than 0.1 micron) to be seen by optical

microscopy. However at the fusion zone and heat-affected zone interface, precipitation was more extensive and accompanied by intergranular cracking. Often these intergranular cracks propagated along the epitaxial columnar grains at the fusion-zone interface. These cracks continued along the columnar-grain boundaries in the fusion zone and finally terminated at the centerline of the weld (Figure 10, Optical Photomicrograph).

In an effort to determine a possible relationship between the intergranular cracks and precipitation in the beryllium, extensive optical and electron metallography was done on the fusion zone–heat-affected zone interface. In addition, electron-microprobe analysis was directed along the beginnings of the intergranular cracks.

The results reveal an association of aluminum-rich areas with the intergranular cracks. For example, Figure 11(a) shows three small cracks along the grain boundaries in the fully recrystallized portion of the heat-affected zone. These particular cracks were chosen for examination because they did not extend into the fusion zone and therefore clearly originated in the heat-affected zone of the electron-beam weld. The intergranular cracks in (a) (marked 1, 2, and 3) are shown again in Figure 11(b) by back-scattered electron analysis with the electron microprobe. A raster scan of aluminum- $K_{\alpha}$  radiation was then performed on this area. Although the data were qualitative, Figure 11(c) shows that aluminum is present along the crack areas.

Furthermore, transmission electron microscopy in the vicinity of microcracks revealed extensive grain-boundary precipitation as illustrated in Figure 12. This observation confirms the association of intergranular cracks in beryllium welds with grain-boundary segregation noted by Hauser and Monroe (3) by replica techniques. Whether or not these aluminum-rich precipitates correspond to their *massive phase* is difficult to determine. Diffraction patterns from these large precipitates were generally complex, but in some instances the particles could be analyzed as of the  $AlMBe_4$  type. On the basis of previous studies (10, 11, and 12) of quenching Rocky Flats Be ingot sheet from above 900 °C, aluminum-rich, grain-boundary precipitates can be expected with moderately rapid cooling rates. Whereas, slower cooling rates permit transition element diffusion to form  $AlMBe_4$  at the grain boundaries in such material.

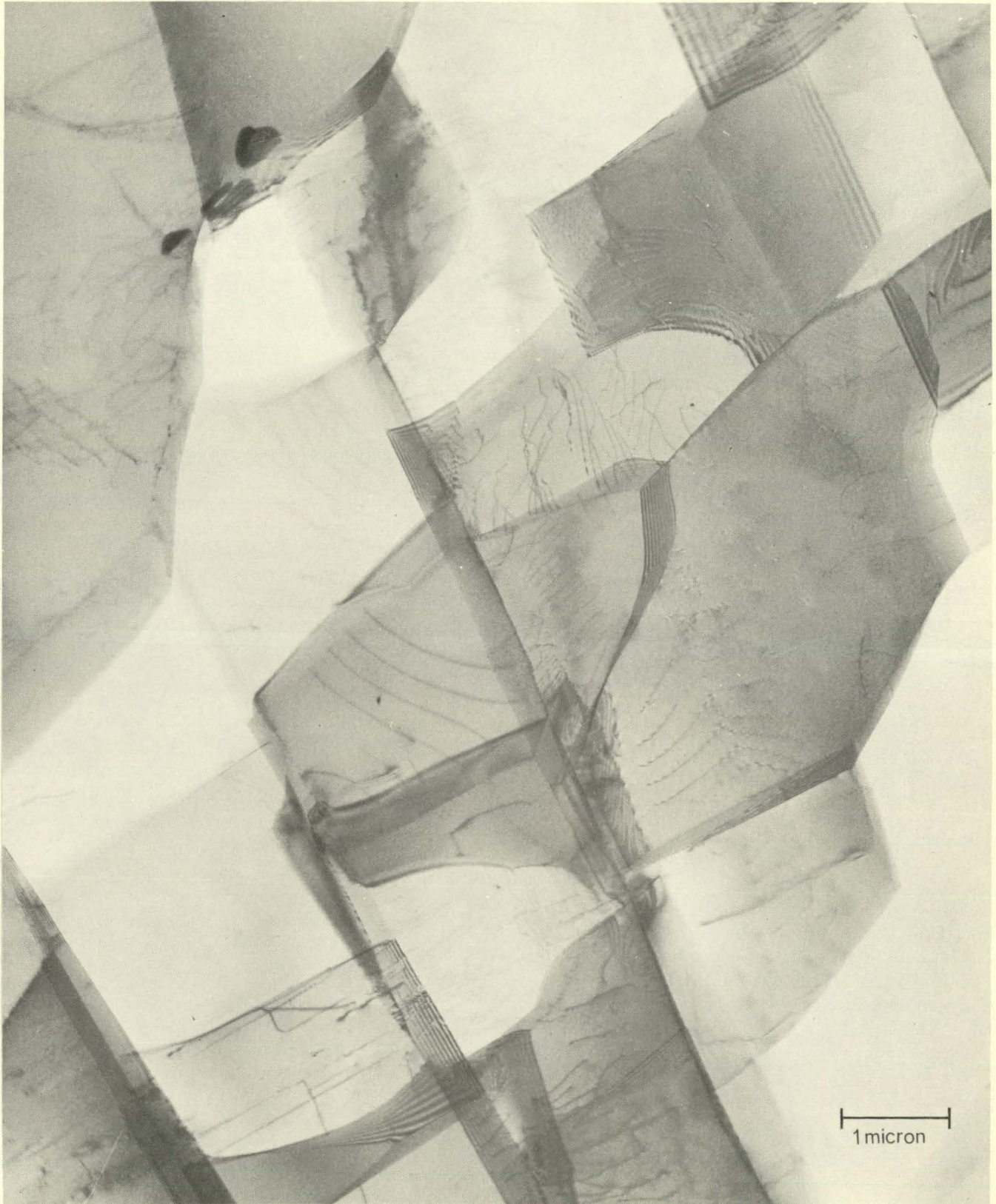


FIGURE 7. Shows Dislocation Arrays and Well Defined Subboundaries as a Result of Polygonization at the Outer Edge of the Heat-Affected Zone.

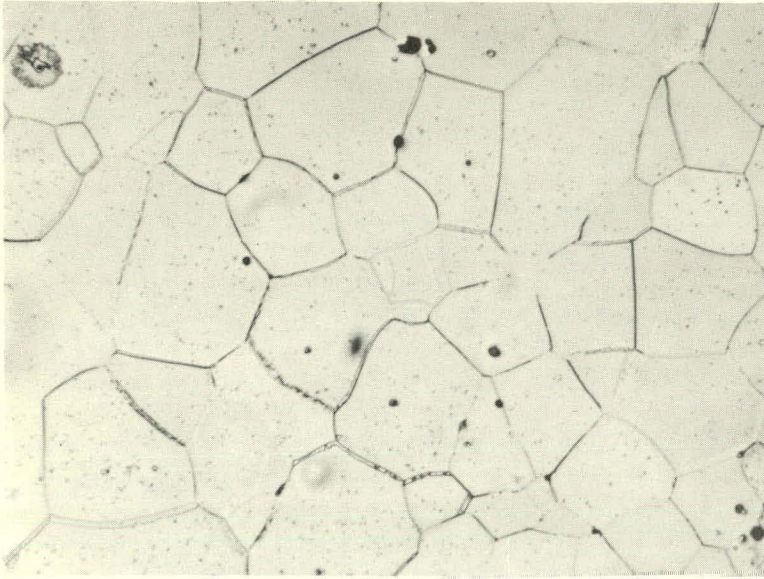
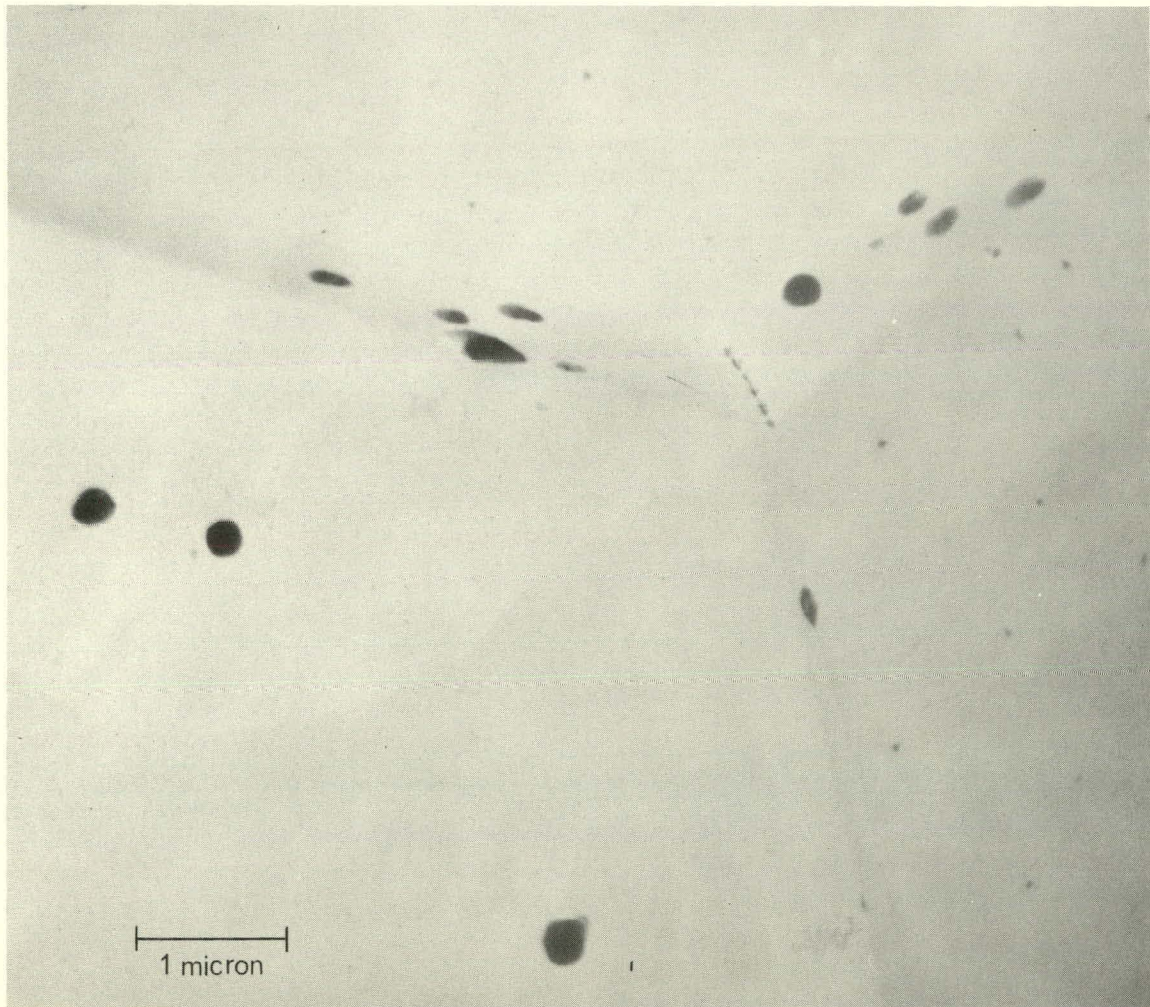


FIGURE 8. Shows Fully Recrystallized Portion of the Heat-Affected Zone. Grain Size is 40 to 75 Microns. (Bright Field, Magnification 300X.)

FIGURE 9. Aluminum-Rich Precipitates in the Matrix and Grain Boundaries of the Recrystallized Zone.





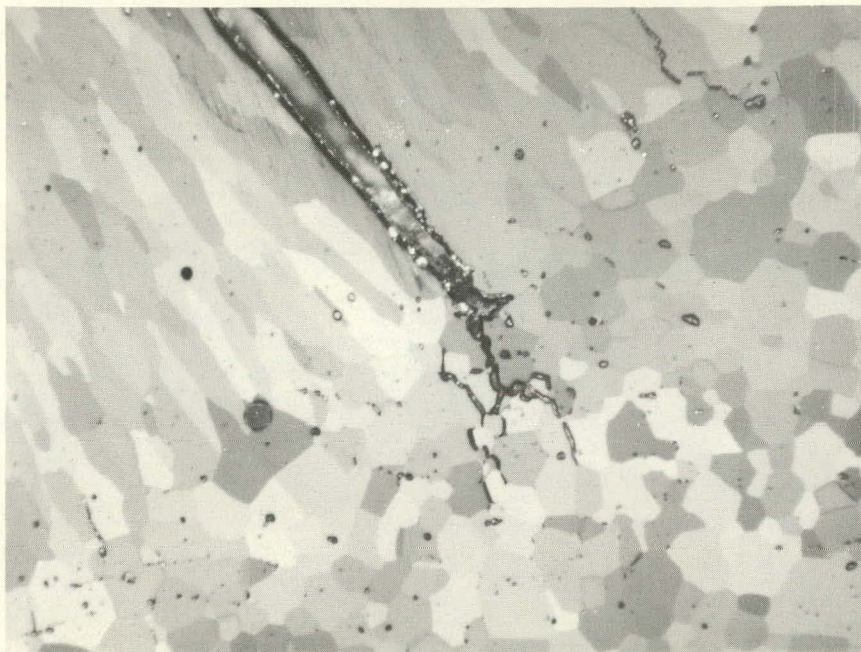


FIGURE 10. Intergranular Cracks in the Heat-Affected Zone. Note that Some of the Cracks Continued to Propagate into the Fusion Zone. (Polarized Light, Magnification 75X.)

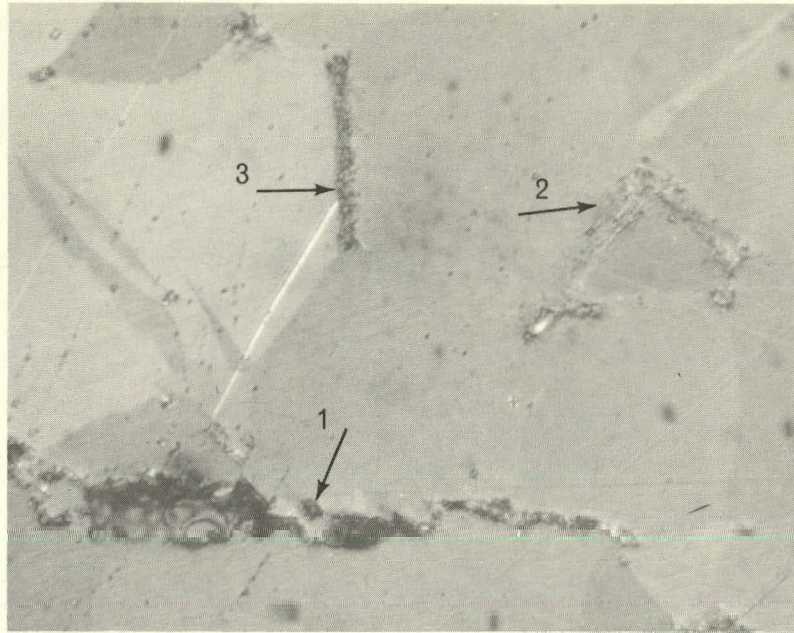
Nonetheless, it is reasonable to assume that these large aluminum-rich precipitates in the grain boundaries of the recrystallized grains introduce *hot-short* liquid areas which, combined with thermal welding stresses, produce the observed intergranular cracking. Although cracks generally originate in the heat-affected zone, the epitaxial relationship of the adjacent fusion-zone grains permits easy propagation of the cracks across the fusion-zone interface. Again it should be emphasized that these cracks were found only in the extremely wide and shallow weld specimens, and can generally be avoided with normal electron-beam welding conditions.

#### Fusion Zone:

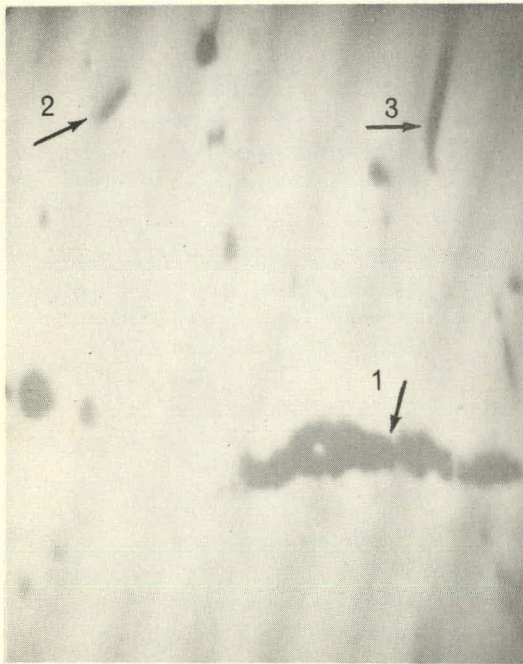
An interesting feature of the fusion zone of the electron-beam welds in the ingot sheet was the appearance after proper electropolishing of *transverse solute bands*. These were more pronounced near the edge of the fusion zone and were approximately normal to the direction of solidification (Figure 13, Optical Photomicrograph). D'Annessa (14) has attributed this phenomenon to cyclic variations in growth rate, resulting from thermal fluctuations

in the weld pool. Therefore it was particularly interesting to directly observe the fusion-zone microstructure by transmission electron microscopy in an effort to identify the origin of these solute bands in Be ingot sheet.

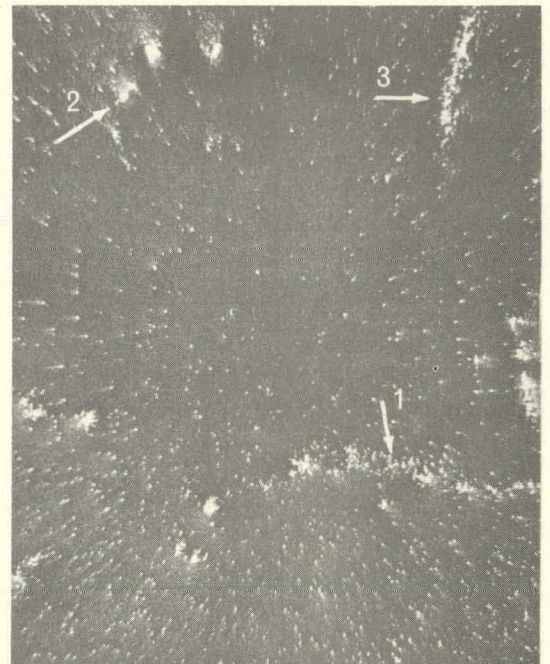
The photomicrographs of the fusion zone revealed that these *solidification bands* consisted of rows of both irregular-shaped and platelet precipitates interconnected by dislocation subboundaries (Figures 14, 15, and 16). The platelet precipitates shown in Figures 14 and 15 reached a length of 2 microns in some instances and were subsequently identified by electron diffraction as the binary compound  $\text{FeBe}_{11}$ . Thus in areas where there was insufficient aluminum to form the ternary  $\text{AlMBe}_4$ , precipitation continued in the form of the binary  $\text{MBe}_{11}$ . Both the rows of precipitates and the interconnecting dislocation tangles preferentially etched during electropolishing to produce the *solute bands*. In the center of the weld, the transverse-solute banding was not as pronounced and Figure 16 reveals that complex precipitation occurred throughout the microstructure. Apparently the periodicity in thermal fluctuations which produces



(a)



(b)



(c)

FIGURE 11. Optical Photomicrograph of Recrystallized Area (a) Showing Three Intergranular Cracks (marked 1, 2, and 3); Same Area (b) as Noted in (a) of Back-Scattered Electron Image on Electron-Microprobe Viewing Screen; and Raster Scan (Aluminum-K<sub>alpha</sub> Radiation) of the Intergranular Crack Area (c).



FIGURE 12. Extensive Aluminum-Rich Precipitation along Grain Boundaries in the Vicinity of Intergranular Cracks in the Heat-Affected Zone.

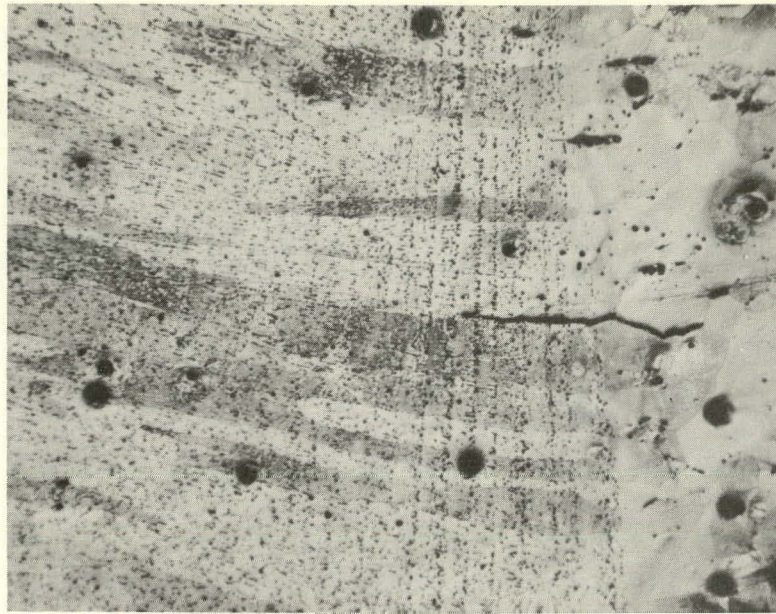
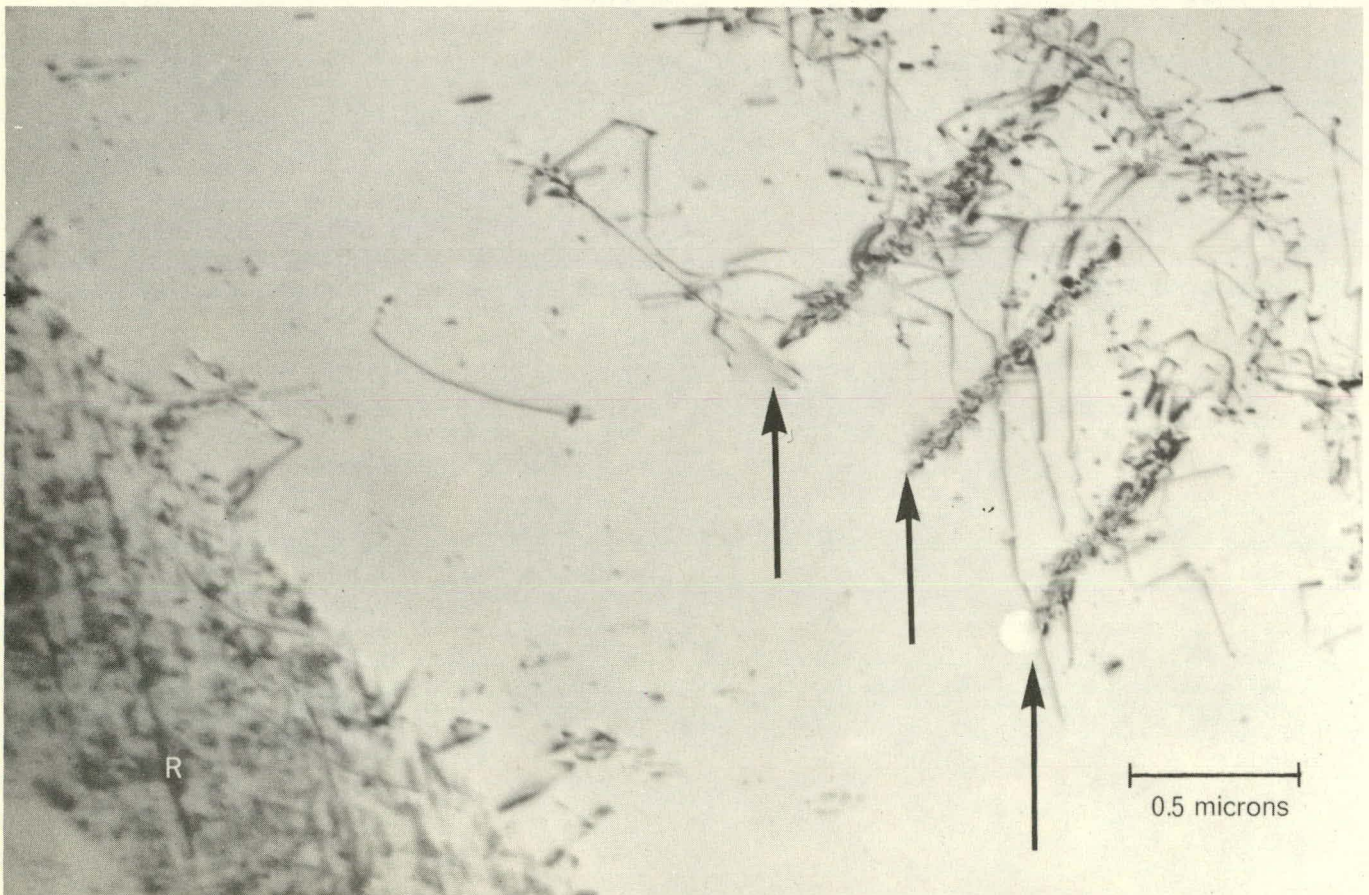


FIGURE 13. Solidification *Bands* across the Columnar Grains near the Edge of the Fusion Zone. Note the Absence of *Banding* in the Heat-Affected Zone at Right. (Bright Field, Magnification 150X.)

FIGURE 14. Row of Platelet-Shaped Precipitates (arrows) Interconnected by Dislocation Tangles. Another Parallel Row is Noted in Region *R*.



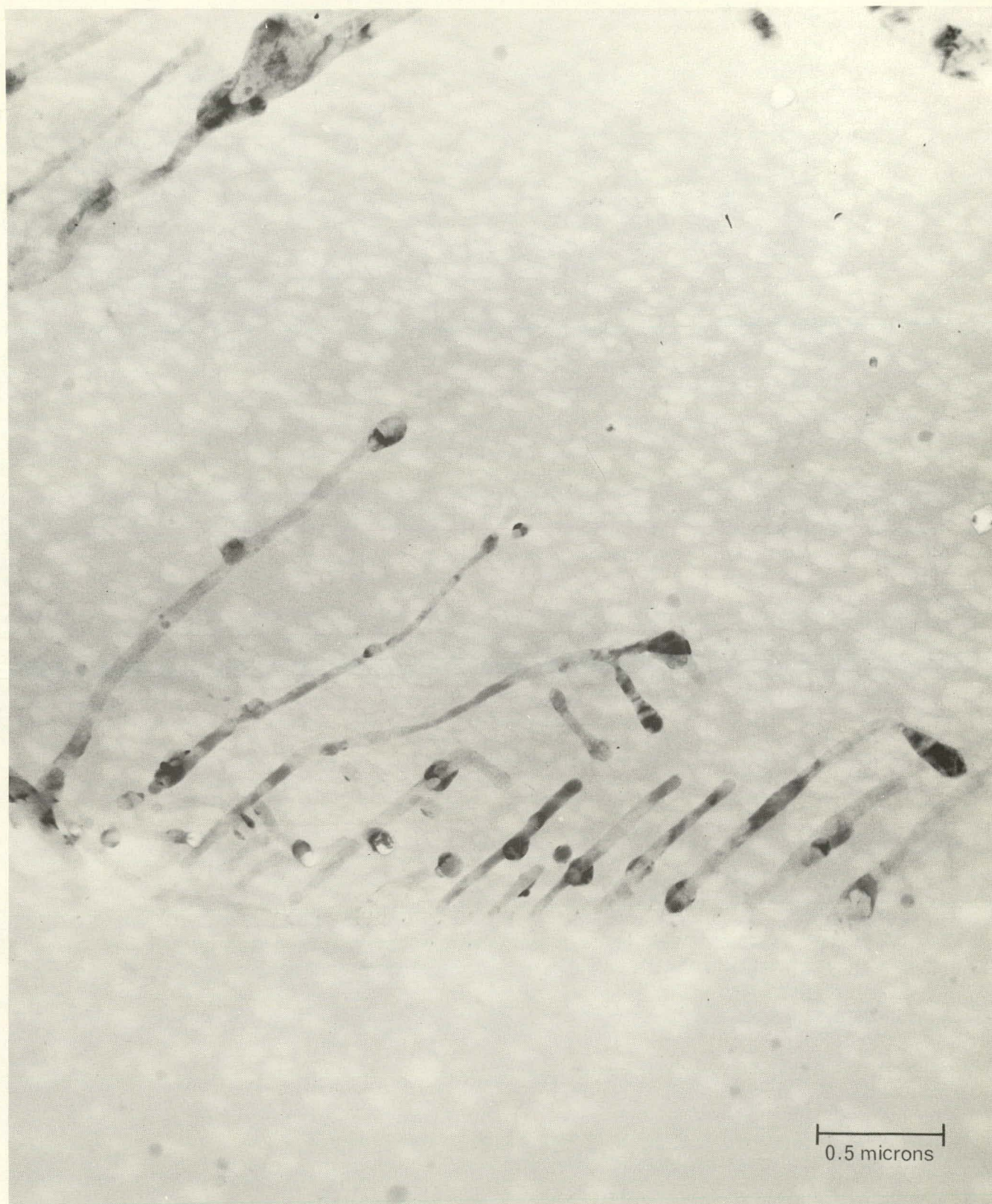


FIGURE 15. Row of Precipitates in the Fusion Zone, Identified by Electron-Diffraction Patterns as  $\text{FeBe}_{11}$ . Dislocations Are Tilted Out of Contrast and Are Not Visible.



FIGURE 16. Complex Precipitation in Center of Fusion Zone of Weld. Note Long Stringer in Columnar-Grain Boundary (arrow).

the solute-enriched bands varies from the center of the weld to the edge of the fusion zone. Hence the precipitates do not form distinct rows, but instead are scattered profusely throughout the matrix and columnar-grain boundaries. Although the precipitates in the center were generally too small to be individually identified by electron-diffraction analysis, the morphology of the precipitates indicates a general mixture of irregular and round  $\text{AlFeBe}_4$  particles, platelets of  $\text{FeBe}_{11}$  and occasional long stringers of  $\text{AlFeBe}_4$ . The long stringers of  $\text{AlFeBe}_4$  were often located in the grain boundaries of the columnar grains, and thus could serve as an additional incentive to intergranular-crack propagation in the fusion zone.

## CONCLUSIONS

The following general conclusions about precipitation in beryllium welds are based on this initial

investigation, using beryllium ingot sheet which had been electron-beam welded to produce wide heat-affected zones and depth-to-width ratios of about 1:1. Hence caution should be used in extending these results to beryllium which is significantly different in impurity content, since the precipitation characteristics may be significantly altered. Nonetheless, the results are generally applicable to the welding of commercial purity beryllium.

1. The predominant precipitates in the fusion zone and the heat-affected zone were identified by electron diffraction as the ternary type,  $\text{AlMBe}_4$ , and the binary type,  $\text{MBe}_{11}$ . (In beryllium of Rocky Flats origin, the predominant transition element,  $\underline{\text{M}}$ , is Fe so that  $\text{AlFeBe}_4$  and  $\text{FeBe}_{11}$  were most often observed in this study.)

2. Transmission electron microscopy revealed extensive aluminum-rich, grain-boundary precipitation in the recrystallized heat-affected zone.
3. Electron-microprobe scanning revealed a high concentration of aluminum in association with intergranular cracks in the recrystallized zone. It is postulated that the aluminum-rich, grain-boundary precipitates introduce *hot-short* liquid areas which produce the intergranular cracking.
4. Transmission photomicrographs indicate that the *solidification* or *solute* bands in the fusion zone consisted of rows of precipitates interconnected by dislocation tangles and sub-boundaries. However the precipitation distribution near the center of the fusion zone becomes more random and complex with the result that banding is not as pronounced.

5. A. Moore. "Improved Mechanical Properties and Associated Constitutional Changes in Commercially Pure Ingot Beryllium as Affected by Heat Treatment above 700 °C." *Journal of Nuclear Metals*, 3:113. 1961.
6. J. A. Carrabine, *et al.* *Beryllium Technology*. L. M. Schetky and H. A. Johnson, Editors. Volume 1, Pages 239-257. Gordon and Breach, Science Publishers, New York. 1966.
7. H. P. Rooksby. "Intermetallic Phases in Commercial Beryllium." *Journal of Nuclear Metals*, 7:205-211. 1962.
8. J. A. Carrabine. "Ternary AlMBe<sub>4</sub> Phases in Commercially Pure Beryllium." *Journal of Nuclear Metals*, 8:278-280. 1963.
9. J. A. Carrabine, *et al.* *Beryllium Technology*. Volume 1. V. D. Scott and H. M. Lindsay, Pages 145-178. Gordon and Breach, Science Publishers, New York. 1966.
10. F. J. Fraikor and V. K. Grotzky. "Grain Boundary Precipitation in Sheet Rolled from Beryllium Ingots." *Transactions of the American Institute of Metallurgical Engineers*, 239:2009-2011. 1967.
11. F. J. Fraikor, *et al.* *Precipitation Characteristics of Rocky Flats Beryllium Ingot Sheet*. RFP-1041. Rocky Flats Division, The Dow Chemical Company, Golden, Colorado. March 12, 1968.
12. F. J. Fraikor and A. W. Brewer. "Precipitation in Quenched and Aged Beryllium Ingot Sheet." *American Society for Metals Transactions Quarterly*. December 1968. (In press.)
13. V. K. Grotzky and F. J. Fraikor. "Bright-Field Optical Microscopy of Beryllium." *Journal of Less Common Metals*, 14:244-246. 1968.
14. A. T. D'Annessa. "Characteristic Redistribution of Solute in Fusion Welding." Research Supplement. *Welding Journal*, 45: 569-S to 576-S. 1966.

## REFERENCES

1. G. K. Hicken and W. B. Sample, Jr. "Joining Beryllium by an Electron Beam Braze Welding Technique." Research Supplement. *Welding Journal*, 46:541-S to 550-S. 1967.
2. D. Hauser, *et al.*, "Electron Beam Welding of Beryllium." Research Supplement. *Welding Journal*, 46:425-S to 540-S. 1967.
3. D. Hauser and R. E. Monroe. "Electron-Beam Welding of Beryllium - Part II." Report No. AFML-TR-66-215. Battelle Memorial Institute, Wright-Patterson Air Force Base, Dayton, Ohio. October 1967.
4. A. W. Jones and R. T. Weiner. "The Effect of Heat Treatment on the Mechanical Properties of Some Commercial Beryllium." *Journal of Less Common Metals*, 6:266-282, 1964.